EBioMedicine 41 (2019) 556–570

Contents lists available at ScienceDirect

EBioMedicine

journal homepage: www.ebiomedicine.com

EBioMedicine
Published by THE LANCET

Cortistatin binds to TNF-α receptors and protects against osteoarthritis

Yunpeng Zhao [a,1], Yuhua Li [a,1], Ruize Qu [b,c,1], Xiaomin Chen [b,c], Wenhan Wang [a,c], Cheng Qiu [c], Ben Liu [a], Xin Pan [a], Liang Liu [d], Krasimir Vasilev [e,g], John Hayball [d], Shuli Dong [f], Weiwei Li [b,*]

[a] Department of Orthopedics, Qilu Hospital, Shandong University, Jinan, Shandong 250012, PR China
[b] Department of Pathology, Qilu Hospital, Shandong University, Jinan, Shandong 250012, PR China
[c] Cheeloo College of Medicine, Shandong University, Jinan, Shandong 250012. PR China
[d] Experimental Therapeutics Laboratory, Hanson Institute and Sansom Institute for Health Research and School of Pharmacy and Medical Sciences, University of South Australia, Adelaide, SA 5000, Australia
[e] Future Industries Institute, University of South Australia, Mawson Lakes, SA 5095, Australia
[f] College of Chemistry, Shandong University, Jinan, Shandong 250101, PR China
[g] School of Engineering, University of South Australia, Mawson Lakes, SA 5095, Australia

ARTICLE INFO

Article history:
Received 3 December 2018
Received in revised form 6 February 2019
Accepted 15 February 2019
Available online 28 February 2019

Keywords:
Osteoarthritis
Chondrocyte
Cortistatin
TNFR
NF-κB signaling

ABSTRACT

Background: Osteoarthritis (OA) is a common degenerative disease, and tumor necrosis factor (TNF-α) is known to play a critical role in OA. Cortistatin (CST) is a neuropeptide discovered over 20 years ago, which plays a vital role in inflammatory reactions. However, it is unknown whether CST is involved in cartilage degeneration and OA development.

Methods: The interaction between CST and TNF-α receptors was investigated through Coimmunoprecipitation and Biotin-based solid-phase binding assay. Western blot, Real-time PCR, ELISA, immunofluorescence staining, nitrite production assay and DMMB assay of GAG were performed for the primary chondrocyte experiments. Surgically induced and spontaneous OA models were established and western blot, flow cytometry, Real-time PCR, ELISA, immunohistochemistry and fluorescence in vivo imaging were performed for in vivo experiments.

Findings: CST competitively bound to TNFR1 as well as TNFR2. CST suppressed proinflammatory function of TNF-α. Both spontaneous and surgically induced OA models indicated that deficiency of CST led to an accelerated OA-like phenotype, while exogenous CST attenuated OA development in vivo. Additionally, TNFR1- and TNFR2-knockout mice were used for analysis and indicated that TNFRs might be involved in the protective role of CST in OA. CST inhibited activation of the NF-κB signaling pathway in OA.

Interpretation: This study provides new insight into the pathogenesis and therapeutic strategy of cartilage degenerative diseases, including OA.

Fund: The National Natural Science Foundation of China, the Natural Science Foundation of Shandong Province, Key Research and Development Projects of Shandong Province and the Cross-disciplinary Fund of Shandong University.

1. Introduction

Osteoarthritis (OA) is a common type of arthritis worldwide. Progressive degeneration and destruction of cartilage are among the characteristics of OA. This disorder has become a prevalent cause of disability in adults which affects millions of people [1,2]. To date, disorganization of chondrocyte metabolism has been reported as one of the causative factors of OA [3,4]. However, the underlying mechanisms of OA remain to be elucidated, and further investigation is required to identify potential treatment strategies [5].

Cortistatin (CST) is a neuropeptide that has multiple functions, especially in inflammatory conditions [6,7]. CST is expressed in various cells and plays a critical role in a number of physiological and disease processes, including cardiac diseases, immune responses and degeneration of the nervous system [8–10]. CST is closely associated with somatostatin in structure and functions, while it was also found to play some different roles compared with somatostatin [11]. Recent data have suggested that CST plays a protective role in inflammatory arthritis mouse models through fighting against inflammation [12]. CST is a type of cyclic peptide that has been reported to bind to several types of receptors [13–15]. Moreover, it has been reported that some cyclic peptides have the ability to bind to TNF-α receptors including TNFR1 and TNFR2

* Corresponding author at: Department of Pathology, Qilu Hospital, Shandong University, 107 Wenhuaxi Road, Jinan 250012, PR China.
E-mail address: liweiweizhao@163.com (W. Li).
[1] These authors contributed equally.

https://doi.org/10.1016/j.ebiom.2019.02.035

Research in context

Evidence before this study

Osteoarthritis is a common degenerative disease all over the world, and reports have shown that tumor necrosis factor (TNF-α) is closely associated with development of OA. Cortistatin (CST) is a multifunctional neuropeptide, and previous reports have proved its role in a number of inflammatory diseases. However, its function in OA, as well as its detailed anti-inflammatory underlying mechanisms remains unidentified.

Added value of this study

In this study, we investigated the interaction between CST and TNF-α receptors, revealing that CST competitively bound to TNFR1 as well as TNFR2. Besides, primary chondrocyte experiments showed that CST suppressed proinflammatory function of TNF-α. Moreover, both spontaneous and surgically induced OA models were established in wild-type and CST-knockout mice. Deficiency of CST led to an accelerated OA-like phenotype, while exogenous CST attenuated OA development in vivo, which was indicated by severity of cartilage destruction and expression level of degenerative biomarkers. Furthermore, TNFR1- and TNFR2-knockout mice were used for analysis and indicated that TNFRs might be involved in the protective role of CST in OA. Additionally, experiments in primary chondrocytes and NF-κB luciferase reporter gene mice revealed that CST inhibited activation of the NF-κB signaling pathway in OA.

Implications of all the available evidence

These findings proved ability of CST to suppress TNF-α induction of inflammation and cartilage degeneration through binding to TNFRs, which maintains homeostasis of chondrocyte in OA. These findings might shed light on treatment of OA in clinic, and provide new insight into the pathogenesis and therapeutic strategy of cartilage degenerative diseases, including OA.

[16,17]. Furthermore, antagonists of the TNF-α/TNFR signaling pathway were reported to have promising anti-inflammatory functions [18,19]. However, whether cyclic neuropeptide CST directly binds to TNFRs is still unknown.

TNF-α is a key inflammatory cytokine [20,21] and plays a predominant role in the inflammation process. TNF-α is known to induce the production of several matrix metalloproteinases, such as MMP-13, ADAMTS-5 and ADAMTS-7, as well as other inflammatory biomarkers [5,22]. TNF-α activates the NF-κB signaling pathway in various conditions, which in turn further facilitates the proinflammatory function of TNF-α [23]. Moreover, recent data suggested that TNF-α was involved in cartilage degeneration in OA development [24]. It was reported that CST associates with TNF-α signaling in inflammatory reactions [25], while the mechanism involved still remains unidentified. Herein, we examined the interaction between CST and TNF-α/TNFR signaling pathway, and determined whether CST is a potential therapeutic strategy against cartilage degeneration during OA development.

2. Results

2.1. CST directly binds to TNF-α receptors and antagonizes the inflammatory function of TNF-α in vitro

It has been reported that proteins binding to TNFRs might exert anti-inflammatory effects through suppressing TNF-α function [26]. This finding, together with the knowledge that cyclic peptides bind to TNFRs [27] and that CST has a cyclic structure [28], prompted us to investigate whether CST binds to TNFRs. Coimmunoprecipitation (Co-IP) was performed in this study to demonstrate the interaction between CST and TNFR1 as well as TNFR2 in human chondrocytes. As shown in Fig. 1A–B, Co-IP indicates that CST interacts with TNFRs. Solid-phase binding is a commonly used assay for direct interaction between different molecules [29]. In the current study, a biotin-based solid-phase binding assay was performed to determine the direct binding between CST and TNFRs. The results (Fig. 1C–D) showed that CST exhibited dose-dependent binding to TNFR1 and TNFR2 compared with the BSA control. To further study whether CST antagonizes binding between TNF-α and TNFRs, we stimulated primary human chondrocytes with biotin-labeled TNF-α in the presence or absence of recombinant CST. As revealed in Fig. 1E, CST dose-dependently diminished the signal of biotin-labeled TNF-α, which is manifested as a leftward shift in the peak in flow cytometry. Moreover, primary chondrocytes were cultured in stimulation with TNF-α, with or without treatment with 50 μg/ml CST, and subjected to Real-time PCR at 24 h time point, or western blotting and ELISA at the 72 h time point. Real-time PCR (Fig. 1F) result showed that TNF-α-mediated production of ADAMTS-5, MMP-13, IL-1β and IL-6 was diminished through treatment of CST. Furthermore, ELISA from conditional medium revealed that CST abolished the elevation of IL-1β and IL-6 induced by TNF-α (Fig. 1G–H). It has been reported that oxidative stress and apoptosis are closely associated with cartilage degeneration, which can be mediated by TNF-α [30]. In this study, Real-time PCR (Fig. 1I) and western blot (Fig. 1K) results indicated that TNF-α promoted the production of the biomarkers of oxidative stress and apoptosis, including COX-2, iNOS, caspase-3, caspase-7 and caspase-9, which were antagonized by CST. The Griess experiment was performed in vitro, and Fig. 1J indicated that the upregulation of nitrite by TNF-α was largely abolished by additional CST treatment. Moreover, flow cytometry was applied to test the apoptosis rate. As shown in Fig. 1L, the apoptosis rate was greatly enhanced with TNF-α stimulation, while CST treatment diminished the apoptosis rate. Additionally, immunofluorescence staining of EdU was conducted to examine DNA replication activity (Fig. 1M and Sup Fig. 1). The results showed that treatment with CST restored cell activity which was reduced by TNF-α stimulation. It was reported that CST binds to somatostatin receptors (Sstrs) which contributes its role in several diseases [31]. In order to exclude the effect of somatostatin receptors for CST function in OA, Octretride, an inhibitor of Sstrs [32], was used along with CST in primary chondrocytes in stimulation of TNF-α. The result showed that effect of CST in chondrocytes was maintained with Octretride application, determined by the diminished expression of degeneration associated molecules, including iNOS, MMP-13 and ADAMTS-5, as detected by western blotting and Real-time PCR (Sup Fig. 2A–B). In summary, CST can directly bind to TNFRs and antagonize the proinflammatory function of TNF-α in chondrocytes.

2.2. CST is expressed in chondrocytes and is decreased during chondrocyte degeneration

To investigate the expression pattern of CST in OA, we collected human cartilage tissue and primary human chondrocytes from patients with OA during arthroplasty surgery as reported [24]. Immunofluorescence and western blotting were conducted in human chondrocytes with or without 10 ng/ml TNF-αstimulation to confirm the expression of CST. Fig. 2A–B showed that TNF-α stimulation reduced CST reproduction in chondrocytes. Articular cartilage from patients with trauma undergoing amputation was used as a control group, and Real-time PCR and western blotting for CST were performed in cartilage samples. Fig. 2C–D revealed that expression level of CST was diminished in OA cartilage. Moreover, destabilization of medial meniscus (DMM) model was established in WT mice, and diminished protein level of CST was

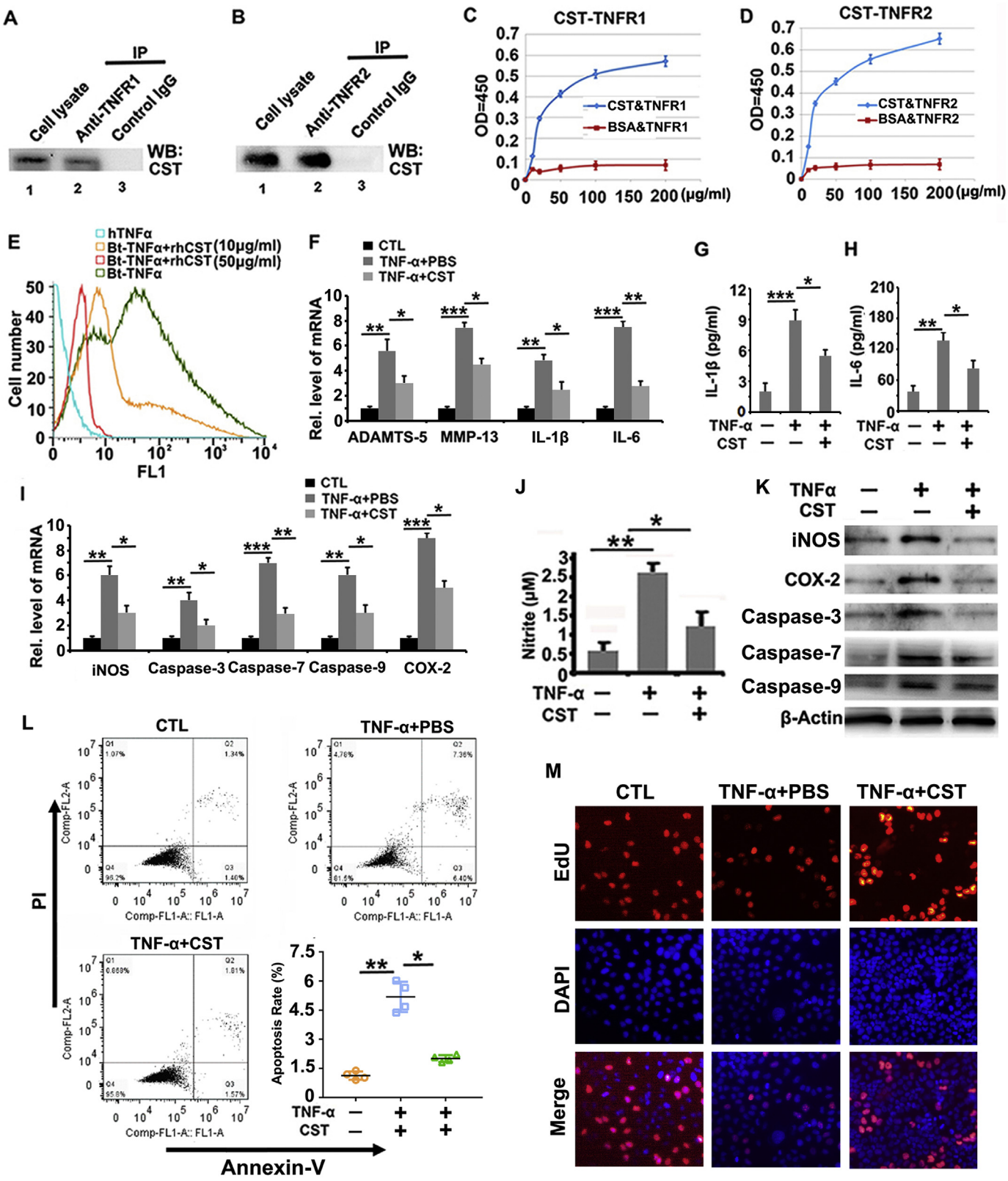

Fig. 1. CST directly binds to TNFR1 and TNFR2 and antagonizes TNF-α function in chondrocytes. (A-B) Detection of the interaction between CST and TNFR in human chondrocytes through Co-IP. (C-D) Examination of the binding affinity between CST and TNFRs with a biotin-based solid-phase binding assay. (E) Treatment with CST remarkably diminished the expression of biotin-TNF-α, as observed through a cell flow cytometry assay. (F) TNF-α-mediated production of ADAMTS-5, MMP-13, IL-1β and IL-6 was diminished through treatment with CST, as determined through Real-time PCR. (G-H) Expression of IL-1β and IL-6 was elevated through the regulation of TNF-α but suppressed by treatment with CST, as determined by ELISA. (I) TNF-α-mediated expression of COX-2, iNOS, caspase-3, caspase-7 and caspase-9 was suppressed by treatment with CST, as detected by Real-time PCR and western blotting. (J) TNF-α-mediated NO production was suppressed by CST, as measured by the Griess assay. (K) CST protected human chondrocytes from negative regulation of TNF-α, as detected by western blotting. (L) The apoptosis rate was enhanced with the stimulation of TNF-α, while CST treatment diminished the apoptosis rate, as detected by flow cytometry. (M) Treatment with CST restored cell activity in stimulation with TNF-α, as detected by immunofluorescence staining. (*$p < .05$, ** $p < .01$, *** $p < .005$ vs control group).

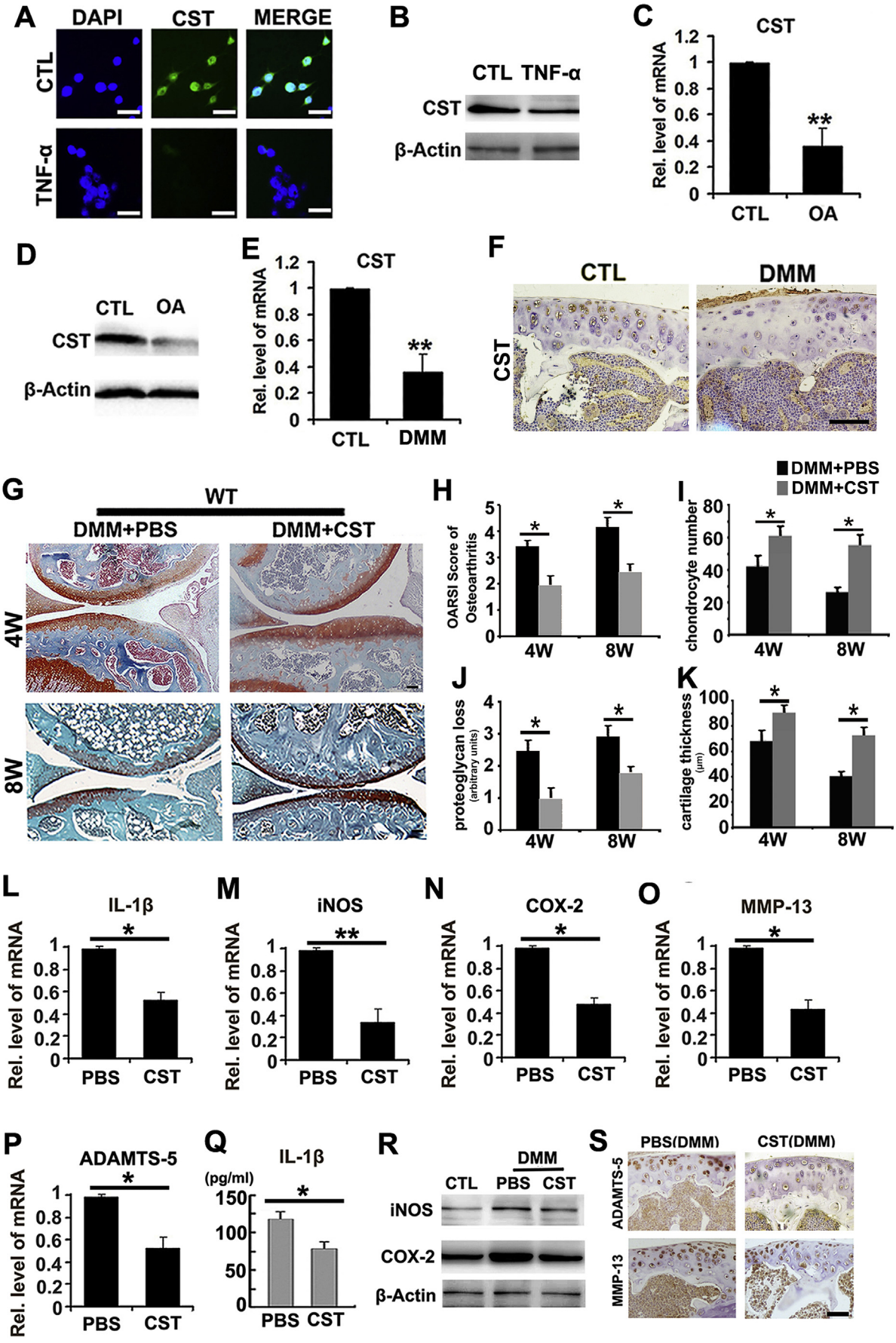
A
DAPI
CST
MERGE
CTL
TNF-α
B
CTL TNF-α
CST
β-Actin
C
CST
Rel. level of mRNA
CTL
OA
D
CTL OA
CST
β-Actin
E
CST
Rel. level of mRNA
CTL
DMM
F
CTL
DMM
CST
G
WT
DMM+PBS
DMM+CST
4W
8W
H
OARSI Score of Osteoarthritis
4W
8W
I
DMM+PBS
DMM+CST
chondrocyte number
4W
8W
J
proteoglycan loss
(arbitrary units)
4W
8W
K
cartilage thickness
(μm)
4W
8W
L
IL-1β
Rel. level of mRNA
PBS
CST
M
iNOS
Rel. level of mRNA
PBS
CST
N
COX-2
Rel. level of mRNA
PBS
CST
O
MMP-13
Rel. level of mRNA
PBS
CST
P
ADAMTS-5
Rel. level of mRNA
PBS
CST
Q
IL-1β
(pg/ml)
PBS CST
R
DMM
CTL PBS CST
iNOS
COX-2
β-Actin
S
PBS(DMM)
CST(DMM)
ADAMTS-5
MMP-13

demonstrated through Real-time PCR and immunohistochemistry (Fig. 2E–F and Sup Fig. 3A).

2.3. CST treatment attenuates the development of the OA phenotype in the DMM model

DMM (destabilization of the medial meniscus) model is a well-established, surgically-induced mice model in OA investigation, and has been extensively studied [34]. To determine whether exogenous CST has protective function against OA, we established DMM model in WT mice ($n = 7$ for each group) and administered intra-articular injections of phosphate buffered saline (PBS) or CST (250 μg/kg body weight) twice a week for 4 weeks or 8 weeks. As shown in Fig. 2G, intra-articular injection of CST remarkably protected the structure of articular cartilage and maintained proteoglycan in the cartilage. OARSI scoring of OA, chondrocyte number, loss of proteoglycan and cartilage thickness were assayed through histology, and CST suppressed OA development (Fig. 2H–K). Moreover, total mRNA was isolated from cartilage at 4 weeks after induction, and levels of OA-associated biomarkers, including IL-1β, iNOS, COX-2, MMP-13 and ADAMTS-5 were assayed through Real-time PCR (Fig. 2L–P and Sup Fig. 4A). Furthermore, serum and cartilage samples were collected at 4 weeks after DMM surgery and subjected to ELISA for IL-1β (Fig. 2Q and Sup Fig. 4B), western blotting for iNOS and COX-2 (Fig. 2R) and immunohistochemistry for ADAMTS-5 as well as MMP-13 (Fig. 2S and Sup Fig. 3B–C). Collectively, CST treatment attenuated the development of OA in the DMM model.

2.4. Deficiency of CST exaggerates the phenotype of OA in aging mice

To study whether loss of CST accelerates degeneration of cartilage, we compared the OA phenotypes of WT and CST−/− mice through aging. Safranin O staining for 10-month old CST−/− mice displayed a remarkably exaggerated loss of proteoglycan in articular cartilage compared with WT littermates (Fig. 3A and Sup Fig. 5A). As a result, the Osteoarthritis Research Society International (OARSI) osteoarthritis score and loss of proteoglycan were enhanced in CST−/− mice compared with WT controls (Fig. 3B–C and Sup Fig. 5B), which indicates that lack of CST leads to more severe structural damage to cartilage. Additionally, the expression of MMP-13 and ADAMTS-5 was examined through immunohistochemistry, and the expression of ADAMTS-5, MMP-13, IL-1β, iNOS and COX-2 was determined by Real-time PCR. Fig. 3D–E and Sup Fig. 5C–D indicated the expression level of the mentioned cytokines were promoted in the cartilage of CST−/− mice compared with WT littermates. To examine the dysfunction of anabolism in OA models, we collected mRNA from the cartilage of each group and performed Real-time PCR for Col2, Aggrecan and Sox-9. As shown in Fig. 3F, Col2, Aggrecan and Sox-9 levels were diminished in CST−/− mice. Besides, total protein extracts from cartilage of 10-month-old WT and CST−/− mice were collected, and western blotting was performed. The results revealed that molecules associated with cartilage degeneration, including ADAMTS-5, MMP-13, iNOS and COX-2, were promoted in CST−/− mice (Fig. 3G). Furthermore, micro-CT scanning (Fig. 3H and Sup Fig. 5I–L), safranin O staining (Fig. 3I) as well as osteophyte scoring of knee joints based on histology (Fig. 3J) revealed significant osteophyte formation and ectopic subchondral bone sclerosis in 10-month-old CST−/− mice. The mRNA extracts from cartilage of 10-month-old WT and CST−/− mice were collected, and Real-time PCR was performed. The results revealed that factors associated with cartilage degeneration, including Col1, ALP, Runx-2, osteocalcin and Axin-2, were enhanced in CST−/− mice (Fig. 3K and Sup Fig. 6A). Additionally, β-catenin, which is reported to be involved in OA, was detected through immunofluorescence, Real-time PCR, western blotting and immunohistochemistry. The results showed that β-catenin expression level was dramatically elevated in 10-month old CST−/− mice, which indicated exaggerated phenotype of OA (Fig. 3L–O, Sup Figs. 5E and 6–C). To testify the alteration of apoptosis in chondrocyte, immunohistochemistry, Real-time PCR and western blot were performed for detection of caspase-3, caspase-7 and caspase-9, and flow cytometry was done for the ratio of Annexin-V positive cells. As shown in Fig. 3P–R, Sup Figs. 5F–H and 6A, the levels of caspase-3, caspase-7 and caspase-9 were upregulated in 10-month-old CST−/− mice. Fig. 3S showed that CST−/− mice exhibited more severe apoptosis than WT mice. Additionally, TRAP staining was conducted in 10-month old WT and CST−/− mice, and CST−/− mice displayed enhanced TRAP expression in subchondral bone (Sup Fig. 5M). This set of experiments implied CST deficiency might accelerate aging procedure in knee joints.

2.5. CST knockout exaggerates OA development in DMM model

To further examine the involvement of CST in OA, DMM OA model was established as previously reported [5] in both CST−/− mice and WT mice. Safranin O staining (Fig. 4A and Sup Fig. 7A) revealed more severe cartilage structure loss in CST−/− mice than in WT mice at the 4-week and 8-week time points. In this study, OARSI scoring of OA, loss of proteoglycan and cartilage thickness were assayed on the basis of histology, demonstrated that CST−/− mice exhibited a more severe OA phenotype than WT group at both time points (Fig. 4B–D and Sup Fig. 7B). Total mRNA was isolated from cartilage 4 weeks after OA induction, and the levels of several OA-associated biomarkers, including MMP-13, ADAMTS-5, iNOS and IL-6, were assayed through Real-time PCR. Fig. 4E–H and Sup Fig. 8A indicated that all the mentioned molecules were enhanced in deficiency of CST. Furthermore, CST deficiency led to increased expression of catabolic and inflammatory molecules in the cartilage of the DMM model, which was assessed through immunohistochemistry for ADAMTS-5 and MMP-13 (Fig. 4I and Sup Fig. 7C–D), western blotting for iNOS (Fig. 4J and Sup Fig. 8B) and ELISA for IL-6 (Fig. 4K and Sup Fig. 8C). To investigate the disorder of anabolism in OA models, we collected mRNA and protein from the cartilage of each group and performed Real-time PCR and western blotting. As shown in Fig. 4L–N, Col2, Aggrecan and Sox-9 levels were diminished in CST−/− mice. Moreover, the expression level of Col2 in the cartilage of the DMM model was detected by western blotting. As revealed in Fig. 4O–P, the Col2 protein level was reduced in CST−/− group.

2.6. CST protects against OA by interacting with TNF-α/TNFR signaling pathway

It is known that TNF-α/TNFR signaling pathway plays a critical role in OA development [34,35]; together with the finding that CST directly binds to TNFRs and antagonizes TNF-α function in chondrocytes, prompted us to demonstrate whether the function of CST in OA is associated with TNFRs. DMM model was established in TNFR1−/−, TNFR2

Fig. 2. The expression pattern of CST in OA and degenerative chondrocytes; CST treatment attenuates the severity of OA in the DMM model. (A-B) CST expression was diminished by TNF-α in chondrocytes, as determined through cell immunostaining and Real-time PCR. (C-D) The expression level of CST was diminished in OA cartilage. Cartilage samples were isolated from patients with or without OA, and Real-time PCR and western blotting were performed. (*E*-F) Levels of CST greatly decreased in DMM models, as observed through Real-time PCR and immunohistochemistry. (G) Intra-articular injection of CST remarkably protected the structure of the articular cartilage and maintained proteoglycan in the cartilage. The DMM model was established in WT mice with or without CST treatment, and the mice were sacrificed at the 4-week and 8-week time points. (H—K) CST suppressed OA development (measured by OARSI scoring), chondrocyte number, loss of proteoglycan (arbitrary units) and cartilage thickness (μm) (measured through histology). (L-P) Levels of OA-associated biomarkers, such as IL-1β, iNOS, COX-2, MMP-13 and ADAMTS-5, were diminished in the CST treatment group as assayed by Real-time PCR. (Q) Decreased IL-1β levels were found with CST treatment in DMM model mice through ELISA. (R) iNOS and COX-2 were found to be suppressed by CST treatment compared to a PBS vehicle control, as detected by western blot. (S) Treatment with CST downregulated the levels of ADAMTS-5 and MMP-13 in DMM model mice, according to immunohistochemical results of articular cartilage ($^{*}p < .05$, $^{**}p < .01$ vs control group). $n = 7$ for each group, Scale bar: 50 μm.

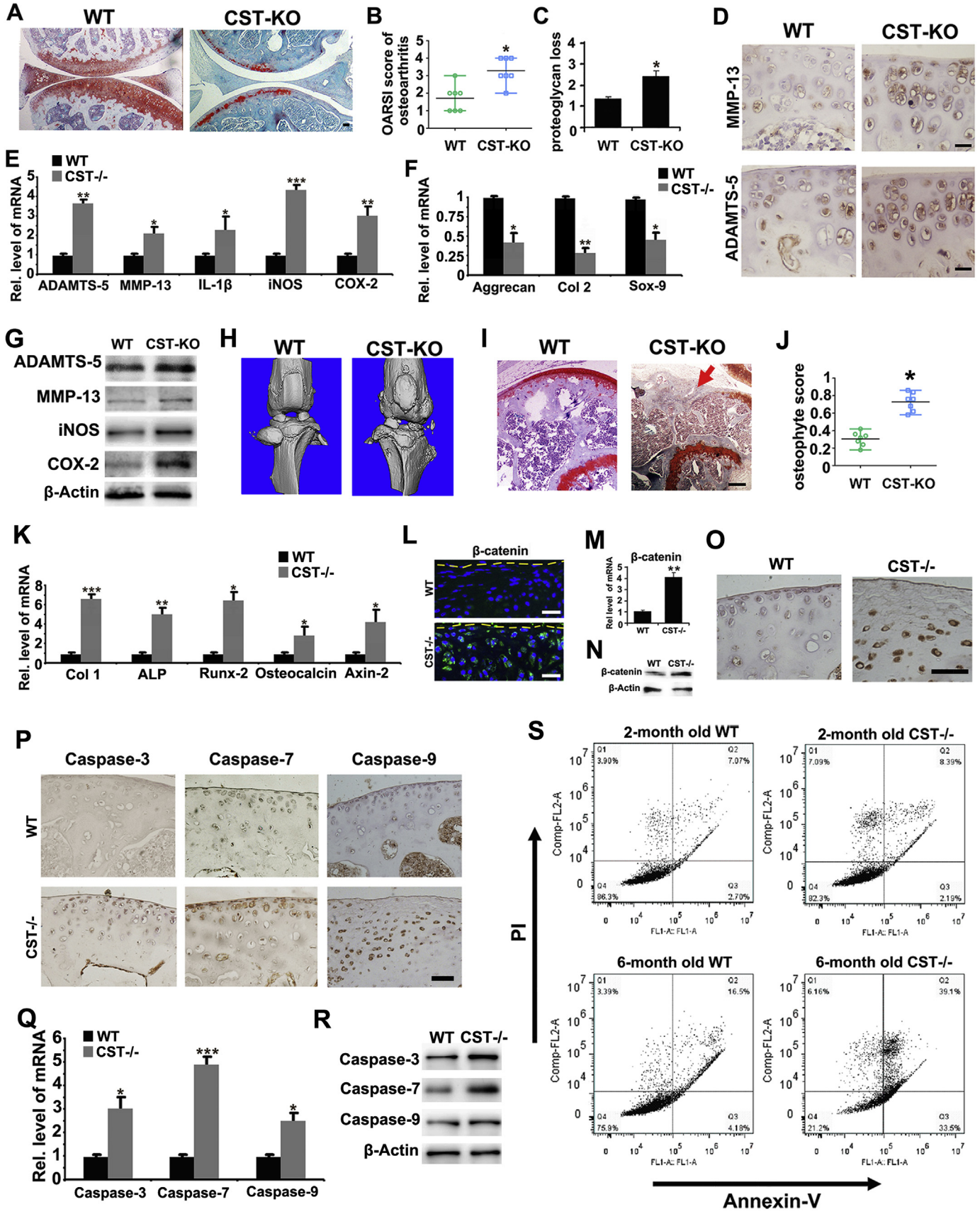
A
WT
CST-KO
B
OARSI score of osteoarthritis
WT
CST-KO
C
proteoglycan loss
WT
CST-KO
D
WT
CST-KO
MMP-13
ADAMTS-5
E
WT
CST-/-
Rel. level of mRNA
ADAMTS-5
MMP-13
IL-1β
iNOS
COX-2
F
WT
CST-/-
Rel. level of mRNA
Aggrecan
Col 2
Sox-9
G
WT
CST-KO
ADAMTS-5
MMP-13
iNOS
COX-2
β-Actin
H
WT
CST-KO
I
WT
CST-KO
J
osteophyte score
WT
CST-KO
K
WT
CST-/-
Rel. level of mRNA
Col 1
ALP
Runx-2
Osteocalcin
Axin-2
L
β-catenin
WT
CST-/-
M
β-catenin
Rel level of mRNA
WT
CST-/-
N
WT
CST-/-
β-catenin
β-Actin
O
WT
CST-/-
P
Caspase-3
Caspase-7
Caspase-9
WT
CST-/-
Q
WT
CST-/-
Rel. level of mRNA
Caspase-3
Caspase-7
Caspase-9
R
WT
CST-/-
Caspase-3
Caspase-7
Caspase-9
β-Actin
S
2-month old WT
2-month old CST-/-
6-month old WT
6-month old CST-/-
PI
Annexin-V
Comp-FL2-A
FL1-A: FL1-A

−/− and TNFR1−/−TNFR2−/− (TNFR1/2−/−) mice, with or without CST treatment. Cartilage tissue was collected at 4-week and 8-week time points, and the OARSI score of OA was assayed on the basis of Safranin O staining. As shown in Fig. 5A–B and Sup Fig. 9A, CST exhibited therapeutic effect in TNFR1−/− as well as TNFR2−/− mice, while the function of CST was largely abolished in TNFR1/2−/− mice. Moreover, mRNA was collected from the cartilage tissue of each group, and Real-time PCR was performed (Fig. 5C–F and Sup Fig. 10A, C, E). CST delivery diminished the expression levels of ADAMTS-5, MMP-13, IL-1β and iNOS in TNFR1−/− and TNFR2−/− mice. However, no significant difference was detected with or without CST treatment in TNFR1/2−/− mice. Moreover, immunohistochemistry was performed for ADAMTS-5, MMP-13 and iNOS, and CST administration reduced the expression signal in TNFR1−/− and TNFR2−/− mice but not TNFR1/2−/− mice (Fig. 5G and Sup Fig. 9B–D). Furthermore, serum and cartilage protein were collected, and ELISA for IL-1β (Fig. 5H) as well as western blotting for iNOS (Fig. 5I–J and Sup Fig. 10B, D, F) was performed. As a result, CST alleviated the expression levels of these degeneration-associated molecules in TNFR1−/− and TNFR2−/− mice but not TNFR1/2−/− mice. This set of experiments suggests that the protective role of CST in OA might be closely associated with its competition with TNF-α to bind to TNFRs.

2.7. CST antagonizes activation of the NF-κB signaling pathway in OA

It is well accepted that NF-κB signaling is activated and plays a critical role in the development of OA [36]. To determine whether CST affects the activity of NF-κB, we stimulated primary human chondrocytes with 10 ng/ml TNF-α in the presence or absence of 50 μg/ml CST. Thereafter, total protein was collected, and CST was found to attenuate pIκB-α and p-p65 expression mediated by TNF-α (Fig. 6A). Moreover, cell immunostaining as well as western blot was performed, and CST antagonized nuclear translocation of NF-κB p65 in chondrocytes (Fig. 6B–C and Sup Fig. 11A). To determine the function of CST in NF-κB activation in vivo, total mRNA and protein extracts were collected from the cartilage of the DMM model. As a result, CST treatment impaired the phosphorylation of IκB-α and p65 (Fig. 6D) in DMM model. Besides, immunohistochemistry of pIκB-α was performed in cartilage tissue of each group, and CST was found to suppress pIκB-α expression (Fig. 6E and Sup Fig. 11B). Furthermore, DMM model was established in WT and CST−/− mice, and cartilage samples were collected at the 4-week time point. Western blotting (Fig. 6F and Sup Fig. 12) and immunohistochemistry (Fig. 6G and Sup Fig. 11C) for pIκB-α and p-p65 suggested that CST deficiency exaggerated NF-κB signaling pathway activity in OA models. Moreover, DMM model was established in NF-κB luciferase reporter mice, and intra-articular injection of CST in the knee joint mitigated the luciferase signal at the 4-week time point (Fig. 6H–I), which indicated repression of NF-κB activation in the DMM model by delivery of exogenous CST.

3. Discussion

OA is characterized by the progressive breakdown of extracellular matrix proteins and the subsequent loss of articular cartilage, which is closely associated with aging process and chronic abrasion of the involved joints [37–39]. Currently, age-dependent spontaneous OA and surgically induced DMM models are well accepted for investigating the pathophysiology of OA [5]. In this study, both types of OA models were used, and CST knockout led to more severe OA, while CST treatment alleviated OA development. Currently, disordered metabolism of chondrocytes is thought to be a key feature of cartilage degeneration and has thus become a focus for investigations concerning OA [40,41]. It is known that stimulation of TNF-α promotes catabolism and suppresses anabolism in chondrocytes, which impairs homeostasis of articular cartilage [5]. Herein, primary human chondrocytes were isolated and cultured, and CST diminished the production of OA-associated molecules induced by TNF-α.

It is well established that exaggerated inflammation is involved in the progression of aging in various systems, such as the nervous system, locomotor system and cardiovascular system, while suppression of inflammatory reactions in cartilage can alleviate the degeneration process [42–44]. Inflammatory biomarkers, including IL-1β, IL-6 and iNOS, are well accepted for their detrimental role in OA development [45, 24, 46]. In this study, CST−/− mice exhibited enhanced levels of these inflammatory molecules, while CST treatment diminished expression level of those cytokines, representing the pivotal role of CST in inflammatory reactions during OA. Additionally, apoptosis is an essential factor of OA [47,48]. In this study, we found that additional application of CST attenuated, while deficiency of CST promoted extent of apoptosis in both in vivo and in vitro experiments, which illustrated potential role of CST in antagonizing apoptosis in OA.

Degradation of the extracellular matrix in cartilage features prominently in the destruction of joint structure, stemming from the enhanced production and secretion of metalloproteinases mainly in chondrocytes [37–39]. It is known that proteoglycan and collagen type 2 are key components of the extracellular matrix in articular cartilage and represent critical parameters in the degeneration of cartilage in OA. ADAMTS-4 and ADAMTS-5 are metalloproteinases that specifically target the degradation of proteoglycan [49]. In addition, MMP-13 directly degrades Col 2 in cartilage [50]. Therefore, the levels of these metalloproteinases, together with the loss of the extracellular matrix, might indicate destruction of cartilage structure and catabolism of chondrocytes during OA development. The findings of this study indicated that loss of CST enhanced, while exogenous CST reduced, production of ADAMTS-5 and MMP-13 in 'aged' and DMM models, respectively, suggesting the potential value of CST in chondrocyte metabolism.

TNF-α is a predominant cytokine that plays a detrimental role in various diseases, including OA [51]. TNF-α participates in inflammation by binding to its receptors, TNFR1 and TNFR2. TNFR1 is expressed in nearly all parts of the body, while TNFR2 is expressed mainly in hematopoietic cells [52]. TNF-α/TNFR signaling is at the top of the proinflammatory cytokine cascade, which has attracted a great deal of attention for its dominance in the pathogenesis of a number of diseases, particularly autoimmune disorders [53]. Molecules competitively binding to TNFRs have been reported to exert therapeutic effects in inflammation by suppressing TNF-α function [54,55]. In the current study, we found that CST

Fig. 3. Deficiency of CST exaggerates the development of spontaneously developed OA. (A) Deficiency of CST caused more loss of proteoglycan in articular cartilage in 10-month-old CST−/− mice than in WT mice as detected by safranin O staining compared. (B, C) A lack of CST exacerbates OARSI scores and OA phenotypes in aging mice. (D) Expression of MMP-13 and ADAMTS-5 greatly increase in CST−/− mice as detected by immunohistochemistry. (E) ADAMTS-5, MMP-13, IL-1β, iNOS and COX-2 were elevated in CST−/− mice as detected by Real-time PCR. (F) Aggrecan, Col-2 and Sox-9 were diminished in CST−/− mice as detected by Real-time PCR. (H) Osteophyte formation and ectopic subchondral sclerosis were detected through micro-CT scanning. (I-J) Safranin O staining and osteophyte score of the knee joint on the basis of histology were examined to detect osteophyte formation (red arrow) and ectopic subchondral sclerosis. (K) Col-1, ALP, Runx-2, osteocalcin and Axin-2 were elevated in CST−/− mice, as detected by Real-time PCR. (L) β-Catenin was elevated in CST−/− mice, as detected by immunofluorescence. (M) β-Catenin was increased in CST−/− mice, as detected by Real-time PCR. (N) β-Catenin was upregulated in CST−/− mice, as detected by western blotting. (O) Expression of β-catenin showed a considerable increase in CST−/− mice, as detected by immunohistochemistry. (P) Expression of caspase-3, caspase-7 and caspase-9 was enhanced in CST−/− mice, as detected by immunohistochemistry. (Q) Caspase-3, caspase-7 and caspase-9 levels increased in CST−/− mice, as detected by Real-time PCR. (P) Secretion of caspase-3, caspase-7 and caspase-9 was upregulated in CST−/− mice by western blotting. (R) CST−/− mice showed substantial apoptosis that increased over time, as detected by flow cytometry. (S) Detection of apoptosis of primary mouse chondrocytes of 2/6-month-old WT/CST−/− mice. ($^{*}p < .05$, $^{**}p < .01$, $^{***}p < .005$ vs control group). n = 7 for each group, Scale bar: 100 μm.

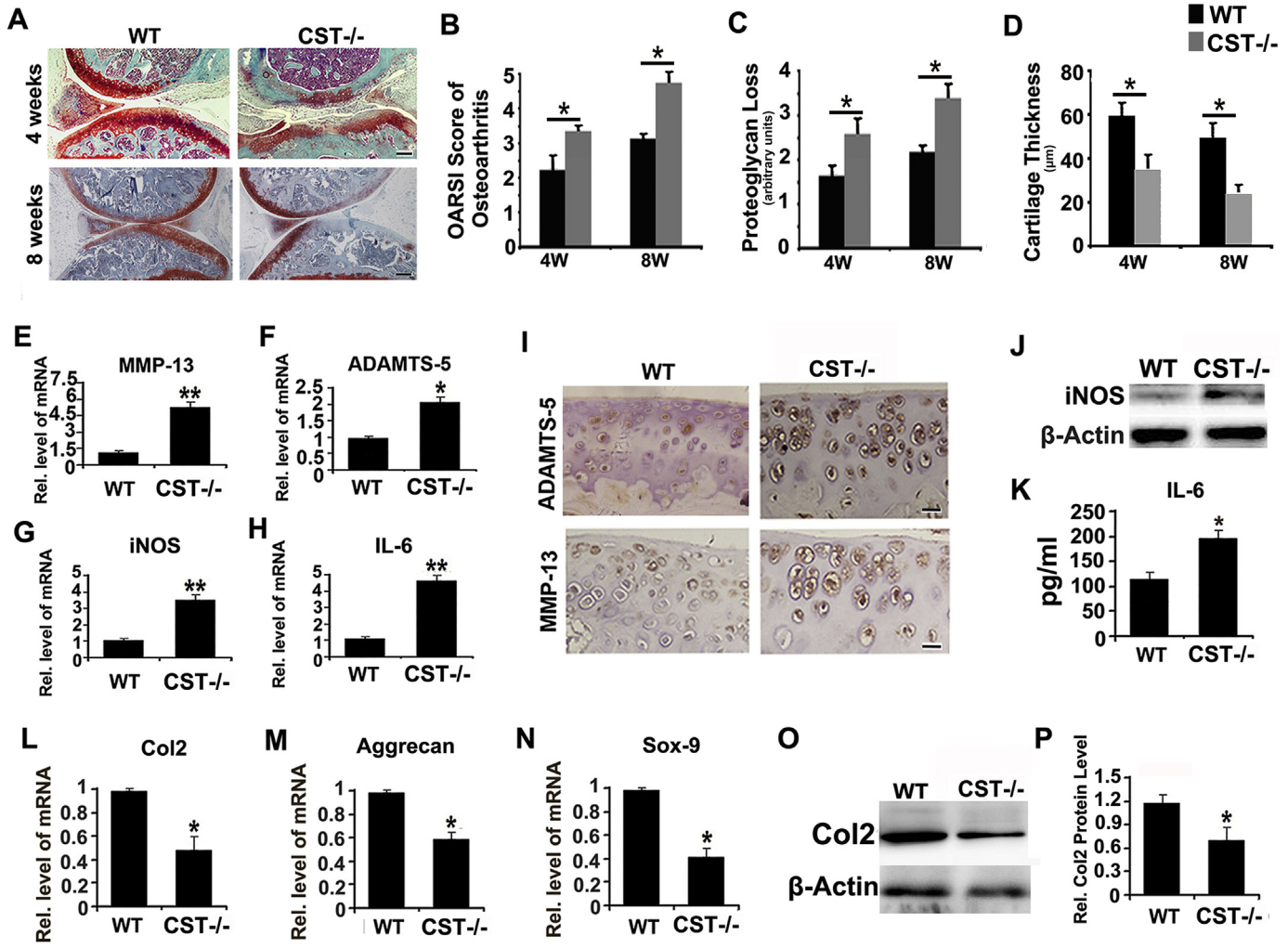

Fig. 4. CST knockout exaggerates OA development in the DMM model. (A) At 4 and 8 weeks, more severe structure loss was present in CST−/− mice than in WT mice as shown through safranin O staining. (B-D) Loss of proteoglycan (arbitrary units) and cartilage thickness (μm) and reduced OARSI scores were detected in CST−/− mice in OA. (E-H) Levels of OA-associated biomarkers MMP-13, ADAMTS-5, iNOS and IL-6 were assayed through Real-time PCR and indicated promotion of CST deficiency. (I) ADAMTS-5 and MMP-13 signals were increased in CST −/− mice, as detected through immunohistochemistry. (J) Increased expression of iNOS was found in CST−/− mice in comparison with WT mice through western blotting. (K) IL-6 was found to be increased in CST−/− mice, as detected by ELISA. (L-N) Col 2, Aggrecan and Sox-9 levels all showed large decreases in CST−/− mice in DMM models through Real-time PCR. (O, P) Col2 was found to decrease greatly in CST−/− mice in DMM models as detected by western blotting (*$p < .01$). n = 7 for each group, Scale bar: 150 μm.

directly binds to TNFRs and antagonizes TNF-α-induced catabolism of chondrocytes in vitro.

Exaggerated catabolism and inflammatory reactions have been extensively studied and widely reported during the development of OA [40,41]. TNF-α induces the expression of molecules associated with OA in human chondrocytes, including ADAMTS-5 and MMP-13, through binding to its receptors TNFR1 and TNFR2 [56]. In addition, the interaction between TNF-α and TNFRs mediates oxidative stress reactions as well as inflammatory responses in various conditions, including OA, during which expression levels of IL-1β, IL-6 and iNOS are enhanced [57]. Herein, we assessed the mentioned biomarkers in TNF-α-induced chondrocytes. As a result, lack of endogenous CST elevated the levels of all these OA-associated molecules, while the additional use of CST remarkably repressed this process. TNFR-knockout mice are commonly used to investigate whether the potential role of some molecules requires interaction with TNFR1 and TNFR2 [5,58]. It has been discovered that CST binds to several types of receptors, including somatostatin receptors (sst2 and sst5) and ghrelin receptors [11,59,60], but the mechanism underlying the role of CST in inflammation as well as immune responses remains to be elucidated. Moreover, the known receptors of CST are seldom reported to be involved in OA. In this study, a commercially available inhibitor of sstrs, Octretride, was used, and CST maintained its effect in TNF-α induction of inflammation in chondrocyte, suggesting sstrs didn't caught much affection to effect of CST in OA. TNF-α is a well-established proinflammatory cytokine in different types of arthritis, which requires its binding to TNF receptors [20,61]. In the current study, CST was found to competitively bind to TNFRs and antagonize TNF-α function in vitro. Treatment with CST was protective in TNFR1−/− and TNFR2−/− mice but not in TNFR1/2−/− mice. Taken together, this information implies that TNFRs are required for the role of CST in cartilage degeneration and development of OA.

The NF-κB signaling pathway plays a key role in facilitating TNF-α function [62,63]. Recent evidence has indicated that the NF-κB signaling pathway is a crucial mediator of age-dependent cartilage degeneration [64,65]. Previous investigations have reported that activation of NF-κB signaling exaggerates, while repression of this signaling alleviates, cartilage degenerative diseases, including OA [34]. Phosphorylation of IκB-α and p65 are known parameters in the activity of the NF-κB signaling pathway [66]. In our research, we detected that the pIκB-α and the p-p65 levels were elevated in TNF-α treated chondrocytes, while this effect was largely antagonized by exogenous CST. Furthermore, nuclear translocation of p65 determines the activity of the NF-κB signaling pathway [67]. In the present study, administration of CST inhibited this

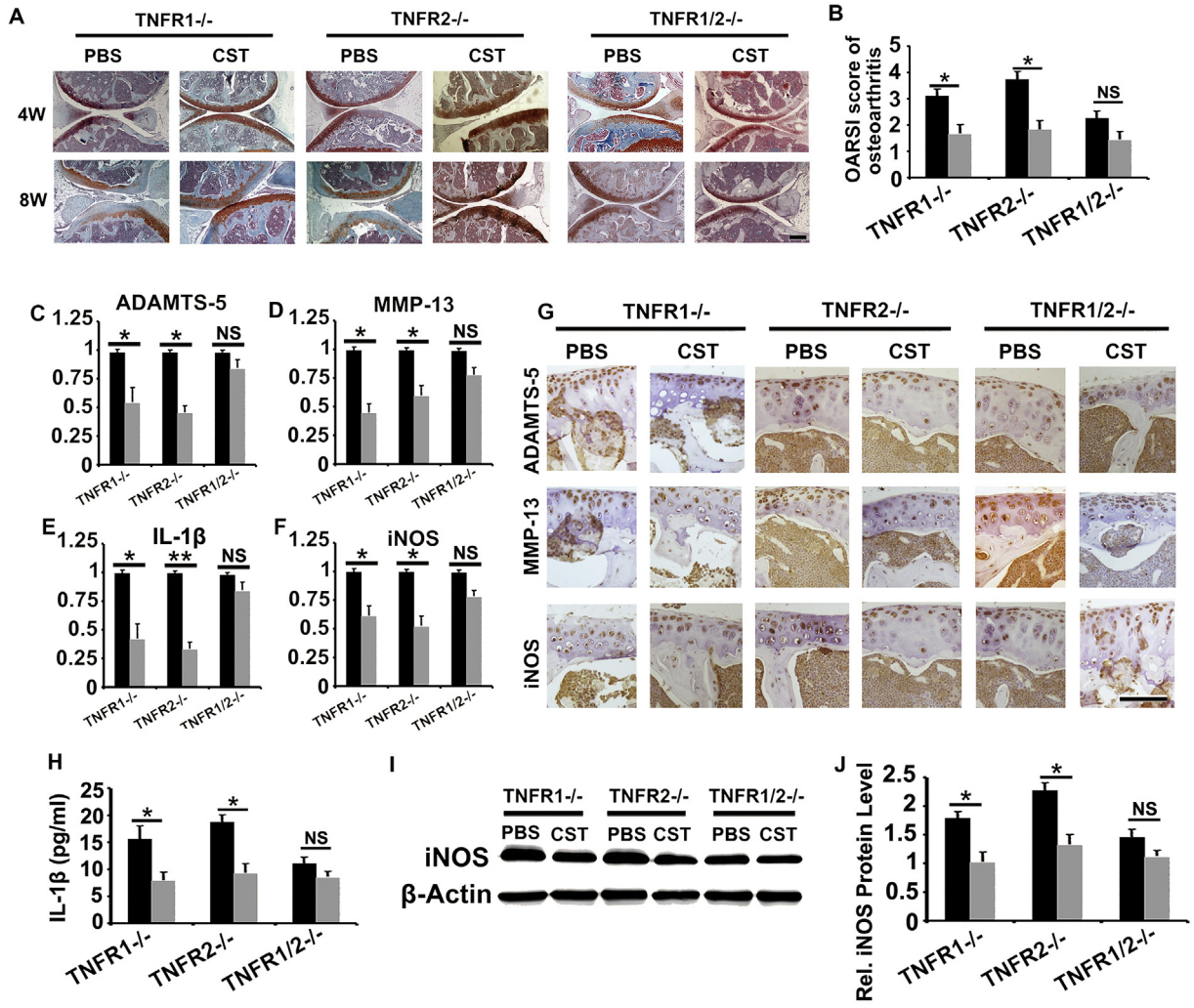

Fig. 5. CST protects against OA development by interacting with the TNF/TNFR signaling pathway. (A, B) Therapeutic effect of CST in TNFR1−/− and TNFR2−/− mice was abolished in TNFR1/2−/− mice, with the detection of Safranin-O staining and OARSI scoring. (C—F) CST delivery diminished expression levels of ADAMTS-5, MMP-13, IL-1β and iNOS in TNFR1−/− and TNFR2−/− mice but showed no difference in TNFR1/2−/− mice as detected through a Real-time PCR assay. (G) ADAMTS-5, MMP-13 and iNOS were diminished with CST treatment in TNFR1−/− and TNFR2−/− mice but not in TNFR1/2−/− mice as determined through immunohistochemistry (of DMM models, at the time of 8 week). (H) ELISA for IL-1β showed the protective effects of CST, but these effects were greatly diminished in TNFR1/2−/− mice. (I-J) Detection of iNOS showed that the levels were all alleviated with CST treatment in TNFR1−/− and TNFR2−/− mice but not in TNFR1/2−/− mice, as assayed by western blotting (*$p < .01$ vs control group). $n = 7$ for each group, Scale bar: 50 μm.

process mediated by TNF-α. Additionally, DMM model was established in NF-κB luciferase reporter gene mice, and treatment with CST abolished the promotion of NF-κB signal in the DMM model. Collectively, these data implied that TNF-αand OA induction of enhanced activation of the NF-κB signaling pathway was repressed by CST, which might contribute to attenuation of cartilage degeneration.

In this study, immunohistochemistry result suggested that CST is expressed in bone marrow cells. It has been reported that some bone marrow hemopoietic cells including osteoclast can express TNFR2 [68], together with the finding that osteoclast is involved in OA development [69] and CST interacts with TNFRs, prompted us to study whether CST affects development of bone marrow derived cells such as osteoclasts. TRAP expression level in bone marrow of CST−/− mice was elevated, which indicated increased osteoclast distribution in CST−/− mice. It might suggest that CST has potential association with osteoclast, while further investigation is required in the future study to deeply elucidate the underlying mechanisms involved.

In summary, a schematic model in Fig. 7 indicates function and mechanism of CST in OA. It's well known that TNF-α can activate NF-κB signaling pathway through binding to its receptors TNFR1 and TNFR2, which consequently leads to phosphorylation of IκBα, and leads to the subsequent nuclear translocation of p65, so as to activate NF-κB signaling [70]. In this study, we found that CST can directly bind to TNFRs, which may be able to antagonize the combination of TNF-α to TNFRs, as a result suppress TNF-α signaling, thus antagonize such process. What's more, in this study, CST antagonized Wnt/β-Catenin signaling, which has been reported to be involved in the development of OA [71]. Therefore, it seems that CST might fight against OA development through multiple mechanisms.

Although a number of in vitro and in vivo experiments were performed to testify the involvement and mechanism of CST in OA, several limitations still exist in this study. Firstly, DMM and age-induced OA models were established, which are extensively studied in OA, while limitations also exist in these two models. DMM model is defined as one of the most usual-used OA models, which have lesions primarily on the central weight-bearing region of the medial tibial plateau and medial femoral condyles, and have no destruction of the subchondral bone [72,73]. However, it can still not naturally reflect human osteoarthritis, which makes it hard to allow the whole disease process to be studied. The age-induced mice OA model is more natural, while may take a long time to induce and the results may be not clear and accurate enough [74,75]. Secondly, in this study we used global CST knockout mice instead of conditional knockout mice. Although the Safranin-O staining for 10-week old WT and CST−/− mice exhibited no significant

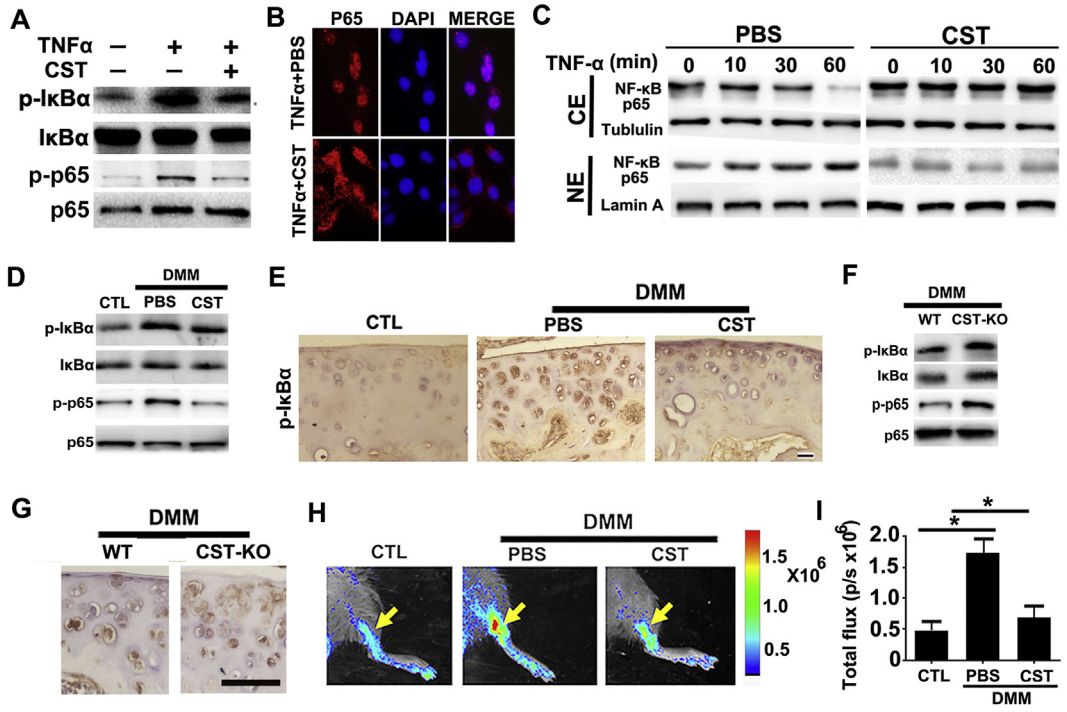

Fig. 6. CST antagonizes NF-κB signaling pathway activation in OA. (A) CST attenuated plκB-α and p-p65 as detected by western blotting after 12-h-stimulation of TNF-α. (B) CST antagonized nuclear translocation of NF-κB p65 in chondrocytes as determined through cell immunostaining after 1-h-stimulation of TNF-α. (C) Nuclear transaction of NF-κB p65 was analyzed by Western blotting. Western blot of NF-κB p65 was performed using cytoplasmic (CE) and nuclear (NE) extracts of 10 ng/ml TNF-α-treated (for 0, 10, 30 and 60 min, respectively) chondrocytes in the presence and absence of 50 μg/ml CST. Tubulin and Lamin A served as cytoplasmic and nuclear controls, respectively. All the mice samples of all gene types and treatment groups in DMM models were detected at the 8th week after operation, before/after sacrifice and sample collection. (D) CST suppressed the phosphorylation of IκB-α and p65 in DMM models as determined through western blotting. (E) CST suppressed plκB-α expression according to immunohistochemistry. (F) Deficiency of CST elevated the level of plκB-α and p-p65 in OA cartilage as determined through western blotting. (G) Immunohistochemistry results showed increased levels of plκB-α in CST−/− mice. (H, I) CST contributed to repression of NF-κB activation in the DMM model in NF-κB luciferase reporter mice. (*p < .05, **p < .01, ***p < .005 vs control group). n = 7 for each group, Scale bar: 150 μm.

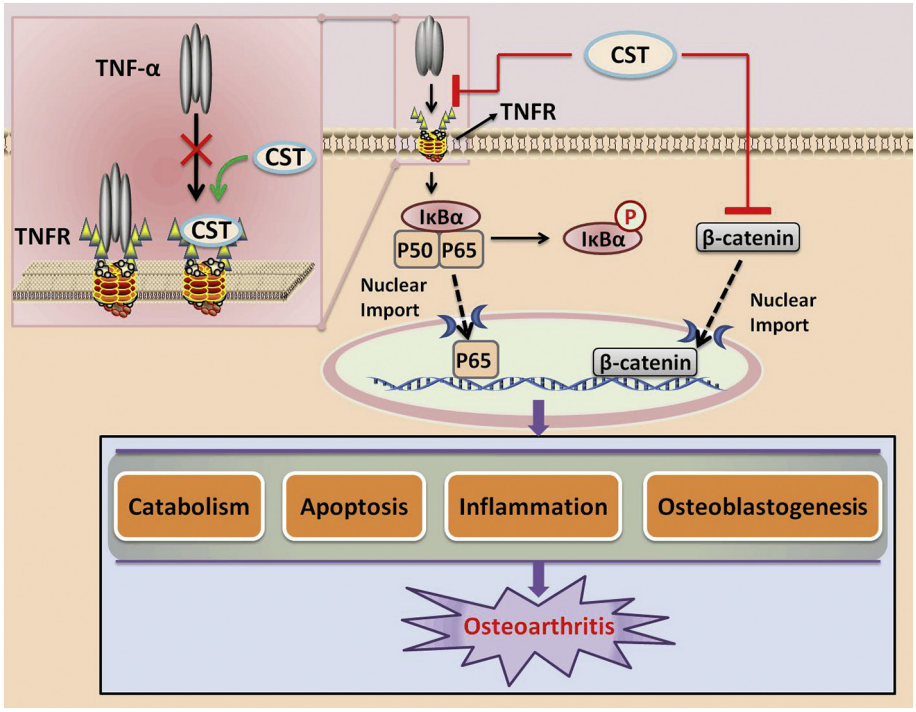

Fig. 7. Schematic depicting proposed effect of CST on OA.

difference in OA phenotype, which might, to some extent, exclude the developmental factor involved in these two genotypes, whether other tissues or other cell types also play a role in OA development of CST−/− group still remain to be further studied. In this study, we excluded female mice to reduce additional variance stemmed from gender difference. However, it makes the study not comprehensive enough, which is required to be further investigated in the future.

Taken together, these results show that CST suppresses TNF-α induction of cartilage degeneration through binding to TNFRs and maintains homeostasis of chondrocytes in OA, which may shed light on potential approaches to treat OA in clinic.

4. Materials and methods

4.1. Mice

All experiments concerning animals in this study were approved by the Institutional Animal Care and Use Committee of Shandong University, and performed according to the ARRIVE guideline [76]. CST−/− mice were established and provided by the National Resource Center of Model Mice (T003038, Nanjing, China). Moreover, 3-month-old C57BL/6 male wild-type (WT) mice, TNFR1−/−, TNFR2−/−, TNFR1−/−/TNFR2−/− (TNFR1/2−/−) mice and NF-κB luciferase reporter gene mice were purchased from Jackson Laboratories for in vivo experiments in this study. Animals of 3 month old between 22~24g of each gene type were chosen, and treated for 7 days in a standard environment (23 ± 2 °C, 12-h light/dark cycle), with water and food supply ad libitum.

4.2. Human cartilage samples

Cartilage samples of human were collected from total knee joint replacement surgery patients for OA. MR Imaging Osteoarthritis Knee Score (MOAKS) was used to analysis the patients' joints, as a semi-quantitative scoring system so as to examine the degree of knee OA [77]. All the experiments were agreed by the ethical review committee of Qilu Hospital, Shandong University, and additionally, the prior informed consent of the patients.

4.3. Primary cultures of human and mouse chondrocytes

Samples of human cartilage were collected from total knee joint replacement surgery patients for OA, with the detection of MOAKS, according to the agreement of the ethical review committee of Qilu Hospital, Shandong University, and the prior informed consent of the patients. Mouse cartilage samples were gathered from knee joints of 2-month-old and 6-month-old WT and CST−/− mice. All experiments were conducted in compliance with the relevant guidelines and regulations. Primary human or mouse articular chondrocytes were collected from the articular cartilage through enzymatic digestion as previously reported [24]. Briefly, cartilage slices were minced and washed clean with 1% PBS, followed by digestion in a mixture of 0.25% collagenase II in FBS-free DMEM with Pen-Strep at 37 °C for 3–5 h in a spinner flask in an incubator with a 5% CO_2 atmosphere. Then, the cell suspension was used to establish cultures in the T175 dishes. At 3–4 days after harvesting, primary chondrocytes were replated at 80% to 85% confluence in 6-well plates and were then used for further studies. Additionally, the chondrocytes were validated through immunofluorescence staining of Aggrecan (Sup Fig. 13).

4.4. DMMB assay of GAG for primary chondrocytes

Mouse primary chondrocytes were cultured as was described above. Primary chondrocytes of each group were moved to tissue-culture flasks with DMEM (containing 25mM HEPES, 2mM glutamine, 100μg/ml streptomycin, 100IU/ml penicillin, 2.5μg/ml gentamicin and without serum), with or without the treatment of 10 ng/ml TNF-α and 50 μg/ml CST. After incubating for 24 h, the conditioned medium was collected for GAG synthesis analysis. Conditioned medium was collected from each experimental group, and the presence of GAG released from primary chondrocytes was quantified using dye DMMB (Polysciences, Warrington, PA, USA). Culture medium was pretreated with 0.5 units/ml of hyaluronidase (Seikagaku, Tokyo, Japan) at 37 °C for 3 h in order to get rid of exogenous HA in order to remove interference. Digests were mixed with DMMB in 96-well plates and read at 520 nm with Spectra Max 384 Microplate Reader (Molecular Devices, Sunnyvale, CA, USA). GAG amount in the conditioned medium was extrapolated with standard chondroitin-6-sulfate sodium salt (Sigma e Aldrich, St. Louis, MO, USA).

4.5. OA models through surgical induction

To demonstrate the protective effect of CST, we placed 3-month-old WT and CST−/− mice under general anesthesia and then subjected them to surgical destabilization of the medial meniscus (DMM) surgery as was previously reported [72] ($n = 25$ for each group). Shortly speaking, the mice were anesthetized with isoflurane, and standard surgical site was prepared. Medial para-patellar arthrotomy was performed at the medial menisco-tibial ligament, which was following transected with curved dissecting forceps. Respective closure of the joint capsule, subcutaneous tissue and skin was then operated. Afterwards, PBS or CST (688,714, GL Biochem(Shanghai) LTD, 10μl each mouse, 250μg/kg body weight) was delivered by intra-articular injection twice a week. Sham surgery was performed on the left knee of each experimental mouse, and on mice of both WT and CST−/− gene type (n = 25, respectively), as was previously reported [24]. To investigate the potential mechanisms for the function of CST in OA, we established a DMM model in 3-month-old TNFR1−/−, TNFR2−/−, TNFR1/2−/− and 3-month-old NF-κB luciferase reporter gene mice, with or without intra-articular injection of CST (250 μg/kg body weight, twice a week) (n = 25 for each group). Sham surgery was performed on mice of each gene type (n = 25, respectively). The mice were given water and food ad libitum, and treated in a standard environment (23 ± 2 °C, 12-h light/dark cycle). 4 or 8 weeks later, the mice were sacrificed, and knee joint tissues were separated and processed for further evaluations. Fourteen mice were used at each time point in each group.

4.6. Histology and immunohistochemistry

The principles of laboratory animal care were carefully followed, and all procedures met the benchmark of the National Institutes of Health guidelines. Every effort was made to minimize suffering. This study was approved by the Animal Experiment Committee of Shandong University.

Mouse knee joints in each experimental group were separated and processed with 4% PFA for 72 h, then decalcified in 10% *w*/*v* EDTA for 14 days, followed by dehydration and embedding in paraffin; subsequently, 5 μm thick sections were cut. Serial sections were taken from each sample and were then stained with safranin O/fast green/iron hematoxylin, as was reported before [34]. Moreover, serial sections of 10-month-old WT and CST−/− mice were stained using tartrate-specific acid phosphatase-positive (TRAP) osteoclasts as previously reported [58,78,79]. Additionally, to examine the indicated biomarkers through immunohistochemistry, we applied 0.1% trypsin for 30 min at 37 °C to pretreat the sections; chondroitinase ABC (Sigma-Aldrich, 0.25 U/ml for 60 min at 37 °C) and hyaluronidase (Sigma-Aldrich, 1 U/ml for 60 min at 37 °C) were used to pretreat the other matrix proteins in the cartilage sections. To reduce nonspecific staining, we applied 10% normal goat serum at room temperature for 30 min for protein blocking. Thereafter, the slices were incubated with anti-MMP13 antibody (diluted 1:200, ab75606, Abcam Corporation, USA), anti-ADAMTS5 antibody (diluted 1:100, ab41037, Abcam Corporation, USA), anti-CST antibody (diluted 1:200, sc-393,108, Santa Cruz Biotechnology, USA),

anti-iNOS antibody (diluted 1:200, ab15323, Abcam Corporation, USA), anti-caspase-3 antibody (diluted 1:150, ab13847, Abcam Corporation, USA), anti-caspase-7 antibody (diluted 1:100, ab25900, Abcam Corporation, USA), anti-caspase-9 antibody (diluted 1:100, ab52298, Abcam Corporation, USA), anti-β-catenin antibody (diluted 1:100, ab32572, Abcam Corporation, USA) and anti-p-IκBα (diluted 1:200, Cell Signaling Technology, USA) at 37 °C for 2 h. The Vectastain Elite ABC kit (Vector, Burlingame, CA) was used for detection, and 0.5 mg/ml 3,3-diaminobenzidine (DAB) in 50 mM Tris-Cl substrate (Sigma-Aldrich) was used for visualization. The sections were then counterstained with 1% hematoxylin. Negative CTL group was set for each antibody (Sup Fig. 15).

4.7. Histopathological and quantificational evaluation of OA

The OARSI histology scoring system was applied as previously reported to grade the proteoglycan content of the articular cartilage on safranin O-stained sections [80]. In the interest of determining whether loss of chondrocytes in cartilage leads to OA changes in mice of each group, articular chondrocytes per unit area were counted, and the average diameter of articular chondrocytes was measured under a microscope at 100×. Adobe Photoshop 7.0 (Adobe Systems) was used to analyze the articular cartilage thickness. Five regions of interest were chosen randomly, and the diameter of each cell within each region of interest was determined from each sample. Each group contained four mice, and the three parameters were determined for each mouse by averaging all sections.

4.8. ELISAs for circulating IL-1β and IL-6

Circulating levels of IL-1β and IL-6 were measured by ELISA in collected serum from mouse OA models in each group [5]. In brief, a commercial kit (eBioscience) was used to assess IL-1β as well as IL-6 according to the manufacturer's instructions. All samples were assayed in triplicate in three mice of each group, and all experiments were repeated at least three times.

4.9. Real-time PCR

Total RNA was extracted from the from knee joint articular cartilage or cultured primary chondrocytes of each experimental group using the RNeasy kit (Qiagen, Valencia, CA, USA) as previously reported [81], and first-strand cDNA was generated using the ImProm-II reverse transcription system (Qiagen, Valencia, CA). Real-time PCR was performed, with SYBR Green I dye used to monitor DNA synthesis. Data from each sample were normalized to GAPDH. Primers used for Real-time PCR were designed to generate products between 100 bp and 200 bp in length. The oligonucleotides used as the specific primers to amplify mouse genes are shown in Table 1. The production of a single specific PCR product was measured through melting curve analysis, and for each indicated molecule, the experiments were repeated three times.

4.10. Western blot analysis

Total protein extracts were collected from human and mouse knee joint articular cartilage or cultured primary chondrocytes. Proteins were resolved on a 10% SDS-polyacrylamide gel and electroblotted onto a nitrocellulose membrane. After being blocked in 5% nonfat dry milk in Tris buffer-saline-TWEEN 20 (10 mM Tris-HCl, pH 8.0; 150 mM NaCl; and 0.5% TWEEN 20), the blots were incubated with polyclonal anti-iNOS (diluted 1:2000, 18,985–1-AP, Proteintech Corporation, USA), anti-COX-2 (diluted 1:1000, ab15191, Abcam Corporation, USA), anti-caspase-3 (diluted 1:1500, ab13847, Abcam Corporation, USA), anti-caspase-7 (diluted 1:1000, ab25900, Abcam Corporation, USA), anti-caspase-9 (diluted 1:1000, ab52298, Abcam Corporation, USA), anti-β-actin (diluted 1:10000, #4967, Cell Signaling Technology, USA), anti-cortistatin (diluted 1:1500, sc-16,743-R, Santa Cruz Biotechnology, USA), anti-ADAMTS5 (diluted 1:1000, ab41037, Abcam Corporation, USA), anti-MMP-13 (diluted 1:1000, 18,165–1-AP, Proteintech Corporation, USA), anti-IκBα (diluted 1:1000, 10,268–1-AP, Proteintech Corporation, USA), anti-p-IκBα (diluted 1:1000, #9244, Cell Signaling Technology, USA), anti-Lamin A (diluted 1:1500, #2032, Cell Signaling Technology, U.S.A.), and anti-Col2 (diluted 1:1000, Santa Cruz Biotechnology, USA) antibodies at 4 °C for 12 h. After a washing step, the horseradish peroxidase-conjugated anti-rabbit secondary antibody (1:2000 dilution) was added to detect all the indicated molecules, and bound antibody was detected with an enhanced chemiluminescence system (Amersham Life Science, Arlington Heights, IL, USA) as reported previously. The expression of cytoplasmic protein was normalized to β-Actin or Lamin A using ImageJ software.

4.11. Coimmunoprecipitation

To examine whether CST interacts with TNF-α receptors, we performed coimmunoprecipitation (Co-IP) as previously reported [66].

Table 1
Primers for real-time PCR.

Source	Name	Forward	Reverse
Human	ADAMTS-5	5′-GAACATCGACCAACTCTACTCCG-3′	5′-CAATGCCCACCGAACCATCT-3′
	MMP-13	5′-ACTGAGAGGCTCCGAGAAATG-3′	5′-GAACCCCGCATCTTGGCTT-3′
	IL-1β	5′-ATGATGGCTTATTACAGTGGCAA-3′	5′-GTCGGAGATTCGTAGCTGGA-3′
	IL-6	5′-ACTCACCTCTTCAGAACGAATTG-3′	5′-CCATCTTTGGAAGGTTCAGGTTG-3′
	iNOS	5′-CAGGGTGTTGCCCAAACTG-3′	5′-GGCTGCGTTCTTCTTTGCT-3′
	Cortistatin	5′-CGGCAGGAATAAGGAAAAGCA-3′	5′-TGGGAGGTCCACTCAAACCA-3′
	Aggrecan	5′-ACTCTGGGTTTTCGTGACTCT-3′	5′-ACACTCAGCGAGTTGTCATGG-3′
	Collagen 2	5′- TGGACGATCAGGCGAAACC-3′	5′- GCTGCGGATGCTCTCAATC -3′
	NF-κB 1	5′-TGGGCACAAGTCGTTTATGA-3′	5′-CTGGAGCCGGTAGGGAAG-3′
	p-IκBα	5′-CATTGGTTCAGAACATGGCCT-3′	5′-AGCTGTTGTGTGCTGAGACTG-3′
	GAPDH	5′-GGAGCGAGATCCCTCCAAAAT-3′	5′-GGCTGTTGTCATACTTCTCATGG-3′
Mouse	ADAMTS-5	5′-CCCAGGATAAAACCAGGCAG-3′	5′-CGGCCAAGGGTTGTAAATGG-3′
	MMP-13	5′-TGTTTGCAGAGCACTACTTGAA-3′	5′-CAGTCACCTCTAAGCCAAAGAAA-3′
	IL-1β	5′-GAAATGCCACCTTTTGACAGTG-3′	5′-TGGATGCTCTCATCAGGACAG-3′
	IL-6	5′-CTGCAAGAGACTTCCATCCAG-3′	5′-AGTGGTATAGACAGGTCTGTTGG-3′
	iNOS	5′-CTCTTCGACGACCCAGAAAAC-3′	5′-CAAGGCCATGAAGTGAGGCTT-3′
	Cortistatin	5′-GAGCGGCCTTCTGACTTTCC-3′	5′-GGGCTTTTTATCCAGGTGTGG-3′
	Aggrecan	5′-CCCAGGATAAAACCAGGCAG-3′	5′-CGGCCAAGGGTTGTAAATGG-3′
	Collagen 2	5′-GGGTCACAGAGGTTACCCAG-3′	5′-ACCAGGGGAACCACTCTCAC-3′
	NF-κB 1	5′-CCTGGAACCACGCCTCTA-3′	5′-GGCTCATATGGTTTCCCATTTA-3′
	p-IκBα	5′-ATGCAGAGTACCACTAACTACCT-3′	5′-CCTCCCCGGATTTCTTGTTTC-3′
	GAPDH	5′-AGCAGTCCCGTACACTGGCAAAC-3′	5′-TCTGTGGTGATGTAAATGTCCTCT-3′

Protein extracts were collected from human articular cartilage, at the concentration of 1μg/μl. Part of the protein was denatured and then used as the input. The protein concentration was measured with a BCA protein assay kit. Protein A/G-agarose beads were added to the protein extracts and incubated for 15 min at 4 °C. The supernatant was collected by centrifugation. Approximately 2.5 μl of anti-CST antibody (diluted 1:1000, sc-16,743-R, Santa Cruz Corporation, USA) was added, and the samples were then incubated for 12 h at 4 °C; normal mouse IgG was used as a negative control. Protein A/G-agarose beads were added and incubated for 2 h at 37 °C. Then, the immunoprecipitated complex was collected by centrifugation and washed 4 times with PBS, after which loading buffer was added. The samples were subjected to western blot analysis.

4.12. Biotin-based solid-phase binding assay

A biotin-based solid-phase binding assay was performed as reported [29]. Briefly, recombinant TNFR1 (50μg/ml) or TNFR2 (50μg/ml) proteins were conjugated with an EZ-Link Sulfo-NHS-Biotinylation Kit (Thermo Scientific, USA). Recombinant CST at a gradient concentration (from 0 to 200μg/ml) was incubated on the ELISA plate, after which biotin-labeled TNFR proteins (Santa Cruz Corporation, USA) were added for combination. Finally, a microplate reader was used to examine the direct interaction of CST/TNFR at an absorbance of 450 nm.

4.13. Flow cytometry assay for apoptosis analysis

Primary human chondrocytes were treated with or without 50 μg/ml CST, along with 10 ng/ml TNF-α, for 48 h. Primary mouse chondrocytes of 2/6-month-old WT or CST−/− mice were cultured without any stimulation, and these cells were harvested for an apoptosis assay. The cells were washed with cold PBS and dissociated into single cells prior to staining with propidium iodide (PI) and FITC Annexin V using the BD Pharmingen FITC Annexin V Apoptosis Detection Kit I (BD Biosciences, USA). Within 1 h of staining, cells were examined by flow cytometry, and data were analyzed using FlowJo.

4.14. Immunofluorescence staining

Primary human chondrocytes were cultured on coverslips and stimulated with 10 ng/ml TNF-α in the presence or absence of 50 μg/ml CST for 1 h. Immunofluorescence staining was performed on these cells and indicated joint tissue with anti-p65 antibody (diluted 1:150, ab86299, Abcam Corporation, USA) or anti-β Catenin antibody (diluted 1:100, ab32572, Abcam Corporation, USA), as described previously, and examined using a confocal fluorescence microscope system [82].

4.15. Fluorescence in vivo imaging system

To assess the protective role of CST in vivo, we imaged anesthetized mice for GFP fluorescence using a whole-body imaging system (IVIS Lumina II, Caliper, France). Filters of 480 nm (±10 nm) and 505 nm (± 5 nm) corresponded to the excitation and emission signals, respectively. High-resolution images were captured directly on a computer and analyzed using Living Image software (Xenogen Corporation, Almeda, California, USA).

4.16. Nitrite production assay

To examine whether CST inhibits TNF-α-mediated inflammatory reactions in chondrocytes, we performed a Griess assay as reported previously [83]. Briefly, primary human chondrocytes were cultured in 96-well flat-bottom plates (1×10^5 cells·well^{-1}) with 10 ng/ml TNF-α (R&D systems) for 24 h in the absence or presence of 50 μg/ml CST. Cell culture supernatants were harvested and tested for NO via the Griess reaction using a commercial kit.

4.17. Statistical analysis

The results are shown as average values±SEM. Student's *t*-test was conducted using SPSS software (SPSS, Chicago, Illinois, USA) for statistical analysis; results were considered statistically significant only when $p < .05$.

Declaration of interests

The authors have declared that no conflict of interest exists.

Author contributions

Conceived and designed the experiments: Weiwei Li, Yunpeng Zhao, John Hayball

Performed the experiments: Ruize Qu, Xiaomin Chen, Ben Liu, Wenhan Wang, Xin Pan, Cheng Qiu.

Analyzed the data: Weiwei Li, Krasimir Vasilev, Liang Liu.

Contributed reagents/materials/analysis tools: Yunpeng Zhao, Yuhua Li, Shuli Dong.

Acknowledgments and funding sources

This work was supported by Key Research and Development Projects of Shandong Province (No. 2015GSF118115), the Natural Science Foundation of Shandong Province (BS2014YY048 and BS2015SW028 to Yunpeng Zhao, and ZR2016HM53 to Yuhua Li), the Cross-disciplinary Fund of Shandong University (Grant No. 2018JC007) and the National Natural Science Foundation of China (81501880 to Yunpeng Zhao and 81602761 to Weiwei Li).

Appendix A. Supplementary data

Supplementary data to this article can be found online at https://doi.org/10.1016/j.ebiom.2019.02.035.

References

[1] DALYs GBD, Collaborators H. Global, regional, and national disability-adjusted life-years (DALYs) for 315 diseases and injuries and healthy life expectancy (HALE), 1990-2015: a systematic analysis for the Global Burden of Disease Study 2015. Lancet 2016;388(10053):1603–58.
[2] Chen D, Xie R, Shu B, et al. Wnt signaling in bone, kidney, intestine, and adipose tissue and interorgan interaction in aging. Ann N Y Acad Sci 2018. https://doi.org/10.1111/nyas.13945 [Epub ahead of print].
[3] Lee CH, Rodeo SA, Fortier LA, Lu C, Erisken C, Mao JJ. Protein-releasing polymeric scaffolds induce fibrochondrocytic differentiation of endogenous cells for knee meniscus regeneration in sheep. Sci Transl Med 2014;6(266):266ra171.
[4] Kong L, Zhao YP, Tian QY, et al. Extracellular matrix protein 1, a direct targeting molecule of parathyroid hormone-related peptide, negatively regulates chondrogenesis and endochondral ossification via associating with progranulin growth factor. FASEB J 2016;30(8):2741–54.
[5] Zhao YP, Liu B, Tian QY, Wei JL, Richbourgh B, Liu CJ. Progranulin protects against osteoarthritis through interacting with TNF-alpha and beta-Catenin signalling. Ann Rheum Dis 2015;74(12):2244–53.
[6] Gonzalez-Rey E, Chorny A, Robledo G, Delgado M. Cortistatin, a new antiinflammatory peptide with therapeutic effect on lethal endotoxemia. J Exp Med 2006;203(3):563–71.
[7] Gonzalez-Rey E, Varela N, Sheibanie AF, Chorny A, Ganea D, Delgado M. Cortistatin, an antiinflammatory peptide with therapeutic action in inflammatory bowel disease. Proc Natl Acad Sci U S A 2006;103(11):4228–33.
[8] Delgado M, Gonzalez-Rey E. Role of cortistatin in the stressed immune system. Front Horm Res 2017;48:110–20.
[9] van Hagen PM, Dalm VA, Staal F, Hofland LJ. The role of cortistatin in the human immune system. Mol Cell Endocrinol 2008;286(1–2):141–7.
[10] Delgado-Maroto V, Falo CP, Forte-Lago I, et al. The neuropeptide cortistatin attenuates experimental autoimmune myocarditis via inhibition of cardiomyogenic T cell-driven inflammatory responses. Br J Pharmacol 2017;174(3):267–80.
[11] Dalm VA, van Hagen PM, van Koetsveld PM, et al. Cortistatin rather than somatostatin as a potential endogenous ligand for somatostatin receptors in the human immune system. J Clin Endocrinol Metab 2003;88(1):270–6.
[12] Gonzalez-Rey E, Chorny A, Del Moral RG, Varela N, Delgado M. Therapeutic effect of cortistatin on experimental arthritis by downregulating inflammatory and Th1 responses. Ann Rheum Dis 2007;66(5):582–8.

[13] Gonzalez-Rey E, Delgado M. Cortistatin as a potential multistep therapeutic agent for inflammatory disorders. Drug News Perspect 2006;19(7):393–9.
[14] Aourz N, Portelli J, Coppens J, et al. Cortistatin-14 mediates its anticonvulsant effects via sst2 and sst3 but not ghrelin receptors. CNS Neurosci Ther 2014;20(7):662–70.
[15] Jiang J, Peng Y, He Z, et al. Intrahippocampal injection of Cortistatin-14 impairs recognition memory consolidation in mice through activation of sst2, ghrelin and GABAA/B receptors. Brain Res 1666;2017:38–47.
[16] Tocker AM, Durocher E, Jacob KD, et al. The scaffolding protein IQGAP1 interacts with NLRC3 and inhibits type I IFN production. J Immunol 2017;199(8):2896–909.
[17] Puga I, Lainez B, Fernandez-Real JM, et al. A polymorphism in the 3′ untranslated region of the gene for tumor necrosis factor receptor 2 modulates reporter gene expression. Endocrinology 2005;146(5):2210–20.
[18] Gladman D, Rigby W, Azevedo VF, et al. Tofacitinib for psoriatic arthritis in patients with an inadequate response to TNF inhibitors. N Engl J Med 2017;377(16):1525–36.
[19] Vermeire S, Sandborn WJ, Danese S, et al. Anti-MAdCAM antibody (PF-00547659) for ulcerative colitis (TURANDOT): a phase 2, randomised, double-blind, placebo-controlled trial. Lancet 2017;390(10090):135–44.
[20] Croft M, Benedict CA, Ware CF. Clinical targeting of the TNF and TNFR superfamilies. Nat Rev Drug Discov 2013;12(2):147–68.
[21] Magis C, van der Sloot AM, Serrano L, Notredame C. An improved understanding of TNFL/TNFR interactions using structure-based classifications. Trends Biochem Sci 2012;37(9):353–63.
[22] Buckland J. Osteoarthritis: positive feedback between ADAMTS-7 and TNF in OA. Nat Rev Rheumatol 2013;9(10):566.
[23] Hayden MS, Ghosh S. Regulation of NF-kappaB by TNF family cytokines. Semin Immunol 2014;26(3):253–66.
[24] Qu R, Chen X, Wang W, et al. Ghrelin protects against osteoarthritis through interplay with Akt and NF-kappaB signaling pathways. FASEB J 2018;32(2):1044–58.
[25] Morell M, Souza-Moreira L, Caro M, et al. Analgesic effect of the neuropeptide cortistatin in murine models of arthritic inflammatory pain. Arthritis Rheum 2013;65(5):1390–401.
[26] Tian Q, Zhao Y, Mundra JJ, et al. Three TNFR-binding domains of PGRN act independently in inhibition of TNF-alpha binding and activity. Front Biosci (Landmark Ed) 2014;19:1176–85.
[27] Ashkenazi A, Marsters SA, Capon DJ, et al. Protection against endotoxic shock by a tumor necrosis factor receptor immunoadhesin. Proc Natl Acad Sci U S A 1991;88(23):10535–9.
[28] Vaudry H, Leprince J, Chatenet D, et al. International Union of Basic and Clinical Pharmacology. XCII. Urotensin II, urotensin II-related peptide, and their receptor: from structure to function. Pharmacol Rev 2015;67(1):214–58.
[29] Tian Q, Zhao S, Liu C. A solid-phase assay for studying direct binding of progranulin to TNFR and progranulin antagonism of TNF/TNFR interactions. Methods Mol Biol 2014;1155:163–72.
[30] Ma CH, Wu CH, Jou IM, et al. PKR activation causes inflammation and MMP-13 secretion in human degenerated articular chondrocytes. Redox Biol 2018;14:72–81.
[31] Broglio F, Papotti M, Muccioli G, Ghigo E. Brain-gut communication: cortistatin, somatostatin and ghrelin. Trends Endocrinol Metab 2007;18(6):246–51.
[32] Carmona Matos DM, Jang S, Hijaz B, et al. Characterization of somatostatin receptors (SSTRs) expression and antiproliferative effect of somatostatin analogues in aggressive thyroid cancers. Surgery 2019;165(1):64–8.
[33] Latourte A, Cherifi C, Maillet J, et al. Systemic inhibition of IL-6/Stat3 signalling protects against experimental osteoarthritis. Ann Rheum Dis 2017;76(4):748–55.
[34] Lai Y, Bai X, Zhao Y, et al. ADAMTS-7 forms a positive feedback loop with TNF-alpha in the pathogenesis of osteoarthritis. Ann Rheum Dis 2014;73(8):1575–84.
[35] Diarra D, Stolina M, Polzer K, et al. Dickkopf-1 is a master regulator of joint remodeling. Nat Med 2007;13(2):156–63.
[36] Minashima T, Zhang Y, Lee Y, Kirsch T. Lithium protects against cartilage degradation in osteoarthritis. Arthr Rheumatol 2014;66(5):1228–36.
[37] Little CB, Hunter DJ. Post-traumatic osteoarthritis: from mouse models to clinical trials. Nat Rev Rheumatol 2013;9(8):485–97.
[38] Kraus VB. Osteoarthritis: the zinc link. Nature 2014;507(7493):441–2.
[39] den Hollander W, Ramos YF, Bomer N, et al. Transcriptional associations of osteoarthritis-mediated loss of epigenetic control in articular cartilage. Arthr Rheumatol (Hoboken, NJ) 2015;67(8):2108–16.
[40] Bouaziz W, Sigaux J, Modrowski D, et al. Interaction of HIF1alpha and beta-catenin inhibits matrix metalloproteinase 13 expression and prevents cartilage damage in mice. Proc Natl Acad Sci U S A 2016;113(19):5453–8.
[41] Huang Z, Kraus VB. Does lipopolysaccharide-mediated inflammation have a role in OA? Nat Rev Rheumatol 2016;12(2):123–9.
[42] Schmidt J, Barthel K, Wrede A, Salajegheh M, Bahr M, Dalakas MC. Interrelation of inflammation and APP in sIBM: IL-1 beta induces accumulation of beta-amyloid in skeletal muscle. Brain 2008;131(Pt 5):1228–40.
[43] Pellegrini C, Fornai M, Colucci R, et al. Alteration of colonic excitatory tachykininergic motility and enteric inflammation following dopaminergic nigrostriatal neurodegeneration. J Neuroinflammation 2016;13(1):146.
[44] Muller AM, Cronen C, Kupferwasser LI, Oelert H, Muller KM, Kirkpatrick CJ. Expression of endothelial cell adhesion molecules on heart valves: up-regulation in degeneration as well as acute endocarditis. J Pathol 2000;191(1):54–60.
[45] Glasson SS, Askew R, Sheppard B, et al. Deletion of active ADAMTS5 prevents cartilage degradation in a murine model of osteoarthritis. Nature 2005;434(7033):644–8.
[46] Orita K, Hiramoto K, Kobayashi H, Ishii M, Sekiyama A, Inoue M. Inducible nitric oxide synthase (iNOS) and alpha-melanocyte-stimulating hormones of iNOS origin play important roles in the allergic reactions of atopic dermatitis in mice. Exp Dermatol 2011;20(11):911–4.
[47] Song J, Baek IJ, Chun CH, Jin EJ. Dysregulation of the NUDT7-PGAM1 axis is responsible for chondrocyte death during osteoarthritis pathogenesis. Nat Commun 2018;9(1):3427.
[48] Onnis A, Cianfanelli V, Cassioli C, et al. The pro-oxidant adaptor p66SHC promotes B cell mitophagy by disrupting mitochondrial integrity and recruiting LC3-II. Autophagy 2018;14(12):2117–38.
[49] Carames B, Hasegawa A, Taniguchi N, Miyaki S, Blanco FJ, Lotz M. Autophagy activation by rapamycin reduces severity of experimental osteoarthritis. Ann Rheum Dis 2012;71(4):575–81.
[50] Otero M, Plumb DA, Tsuchimochi K, et al. E74-like factor 3 (ELF3) impacts on matrix metalloproteinase 13 (MMP13) transcriptional control in articular chondrocytes under proinflammatory stress. J Biol Chem 2012;287(5):3559–72.
[51] Rhee J, Park SH, Kim SK, et al. Inhibition of BATF/JUN transcriptional activity protects against osteoarthritic cartilage destruction. Ann Rheum Dis 2017;76(2):427–34.
[52] Luo D, Luo Y, He Y, et al. Differential functions of tumor necrosis factor receptor 1 and 2 signaling in ischemia-mediated arteriogenesis and angiogenesis. Am J Pathol 2006;169(5):1886–98.
[53] Aggarwal BB. Signalling pathways of the TNF superfamily: a double-edged sword. Nat Rev Immunol 2003;3(9):745–56.
[54] Al-Lamki RS, Mayadas TN. TNF receptors: signaling pathways and contribution to renal dysfunction. Kidney Int 2015;87(2):281–96.
[55] Liu CJ, Bosch X. Progranulin: a growth factor, a novel TNFR ligand and a drug target. Pharmacol Ther 2012;133(1):124–32.
[56] Yamamoto K, Okano H, Miyagawa W, et al. MMP-13 is constitutively produced in human chondrocytes and co-endocytosed with ADAMTS-5 and TIMP-3 by the endocytic receptor LRP1. Matrix Biol 2016;56:57–73.
[57] Hu J, Yan Q, Shi C, Tian Y, Cao P, Yuan W. BMSC paracrine activity attenuates interleukin-1beta-induced inflammation and apoptosis in rat AF cells via inhibiting relative NF-kappaB signaling and the mitochondrial pathway. Am J Transl Res 2017;9(1):79–89.
[58] Zhao YP, Tian QY, Frenkel S, Liu CJ. The promotion of bone healing by progranulin, a downstream molecule of BMP-2, through interacting with TNF/TNFR signaling. Biomaterials 2013;34(27):6412–21.
[59] Duran-Prado M, Morell M, Delgado-Maroto V, et al. Cortistatin inhibits migration and proliferation of human vascular smooth muscle cells and decreases neointimal formation on carotid artery ligation. Circ Res 2013;112(11):1444–55.
[60] Morell M, Camprubi-Robles M, Culler MD, de Lecea L, Delgado M. Cortistatin attenuates inflammatory pain via spinal and peripheral actions. Neurobiol Dis 2014;63:141–54.
[61] Dong Y, Fischer R, Naude PJ, et al. Essential protective role of tumor necrosis factor receptor 2 in neurodegeneration. Proc Natl Acad Sci U S A 2016;113(43):12304–9.
[62] Jeon M, Han J, Nam SJ, Lee JE, Kim S. Elevated IL-1beta expression induces invasiveness of triple negative breast cancer cells and is suppressed by zerumbone. Chem Biol Interact 2016;258:126–33.
[63] Rosebeck S, Rehman AO, Apel IJ, et al. The API2-MALT1 fusion exploits TNFR pathway-associated RIP1 ubiquitination to promote oncogenic NF-kappaB signaling. Oncogene 2014;33(19):2520–30.
[64] Toegel S, Weinmann D, Andre S, et al. Galectin-1 couples glycobiology to inflammation in osteoarthritis through the activation of an NF-kappaB-regulated gene network. J Immunol 2016;196(4):1910–21.
[65] Greene MA, Loeser RF. Aging-related inflammation in osteoarthritis. Osteoarthr Cartil 2015;23(11):1966–71.
[66] Tang W, Lu Y, Tian QY, et al. The growth factor progranulin binds to TNF receptors and is therapeutic against inflammatory arthritis in mice. Science 2011;332(6028):478–84.
[67] Campbell KA, Minashima T, Zhang Y, et al. Annexin A6 interacts with p65 and stimulates NF-kappaB activity and catabolic events in articular chondrocytes. Arthritis Rheum 2013;65(12):3120–9.
[68] Gerstenfeld LC, Cho TJ, Kon T, et al. Impaired fracture healing in the absence of TNF-alpha signaling: the role of TNF-alpha in endochondral cartilage resorption. J Bone Miner Res 2003;18(9):1584–92.
[69] Aso K, Shahtaheri SM, Hill R, Wilson D, McWilliams DF, Walsh DA. Associations of symptomatic knee OA with histopathologic features in subchondral bone. Arthr Rheumatol 2019. https://doi.org/10.1002/art.40820 Epub ahead of print.
[70] Zhao J, Zhang L, Mu X, et al. Development of novel NEMO-binding domain mimetics for inhibiting IKK/NF-kappaB activation. PLoS Biol 2018;16(6):e2004663.
[71] Liu Y, Lin F, Fu Y, et al. Cortistatin inhibits arterial calcification in rats via GSK3beta/beta-catenin and protein kinase C signalling but not c-Jun N-terminal kinase signalling. Acta Physiol (Oxf) 2018;223(3):e13055.
[72] Glasson SS, Blanchet TJ, Morris EA. The surgical destabilization of the medial meniscus (DMM) model of osteoarthritis in the 129/SvEv mouse. Osteoarthr Cartil 2007;15(9):1061–9.
[73] Chinzei N, Rai MF, Hashimoto S, et al. Evidence for genetic contribution to variation in posttraumatic osteoarthritis in mice. Arthritis Rheumatol 2018. https://doi.org/10.1002/art.40730 Epub ahead of print.
[74] Cope PJ, Ourradi K, Li Y, Sharif M. Models of osteoarthritis: the good, the bad and the promising. Osteoarthr Cartil 2019;27(2):230–9.
[75] Choi WS, Yang JI, Kim W, et al. Critical role for arginase II in osteoarthritis pathogenesis. Ann Rheum Dis 2019. https://doi.org/10.1136/annrheumdis-2018-214282 Epub ahead of print.
[76] Kilkenny C, Browne W, Cuthill IC, et al. Animal research: reporting in vivo experiments–the ARRIVE guidelines. J Cereb Blood Flow Metab 2011;31(4):991–3.

[77] Roze RH, Bierma-Zeinstra SM, Agricola R, Oei EH, Waarsing JH. Differences in MRI features between two different osteoarthritis subpopulations: data from the Osteoarthritis Initiative. Osteoarthr Cartil 2016;24(5):822–6.
[78] Zhao YP, Wei JL, Tian QY, et al. Progranulin suppresses titanium particle induced inflammatory osteolysis by targeting TNFalpha signaling. Sci Rep 2016;6:20909.
[79] Zhao YP, Tian QY, Liu B, et al. Progranulin knockout accelerates intervertebral disc degeneration in aging mice. Sci Rep 2015;5:9102.
[80] Glasson SS, Chambers MG, Van Den Berg WB, Little CB. The OARSI histopathology initiative - recommendations for histological assessments of osteoarthritis in the mouse. Osteoarthr Cartil 2010;18(Suppl. 3):S17–23.
[81] Li W, Wu X, Qu R, et al. Ghrelin protects against nucleus pulposus degeneration through inhibition of NF-kappaB signaling pathway and activation of Akt signaling pathway. Oncotarget 2017;8(54):91887–901.
[82] Li W, Zhao Y, Xu X, et al. Rebamipide suppresses TNF-alpha mediated inflammation in vitro and attenuates the severity of dermatitis in mice. FEBS J 2015;282(12):2317–26.
[83] Li W, Wu X, Xu X, et al. Coenzyme Q10 suppresses TNF-alpha-induced inflammatory reaction in vitro and attenuates severity of dermatitis in mice. Inflammation 2016;39(1):281–9.